AFRL-RV-PS-
TR-2013-0163

THERMOSPHERIC MASS DENSITY SPECIFICATION: SYNTHESIS OF OBSERVATIONS AND MODELS

Tomoko Matsuo and Delores J. Knipp

Regents of the University of Colorado
The Office of Contracts and Grants
3100 Marine Street, Room 479, UCB
Boulder, CO 80303-1058

21 October 2013

Final Report

APPROVED FOR PUBLIC RELEASE; DISTRIBUTION IS UNLIMITED.

AIR FORCE RESEARCH LABORATORY
Space Vehicles Directorate
3550 Aberdeen Ave SE
AIR FORCE MATERIEL COMMAND
KIRTLAND AIR FORCE BASE, NM 87117-5776

DTIC COPY

NOTICE AND SIGNATURE PAGE

Using Government drawings, specifications, or other data included in this document for any purpose other than Government procurement does not in any way obligate the U.S. Government. The fact that the Government formulated or supplied the drawings, specifications, or other data does not license the holder or any other person or corporation; or convey any rights or permission to manufacture, use, or sell any patented invention that may relate to them.

This report was cleared for public release by the 377 ABW Public Affairs Office and is available to the general public, including foreign nationals. Copies may be obtained from the Defense Technical Information Center (DTIC) (http://www.dtic.mil).

AFRL-RV-PS-TR-2013-0163 HAS BEEN REVIEWED AND IS APPROVED FOR PUBLICATION IN ACCORDANCE WITH ASSIGNED DISTRIBUTION STATEMENT.

//SIGNED//	//SIGNED//
Dr. Chin Lin	Edward J. Masterson, Colonel, USAF
Program Manager, AFRL/RVBXI	Chief, Battlespace Environment Division

This report is published in the interest of scientific and technical information exchange, and its publication does not constitute the Government's approval or disapproval of its ideas or findings.

REPORT DOCUMENTATION PAGE

Form Approved
OMB No. 0704-0188

Public reporting burden for this collection of information is estimated to average 1 hour per response, including the time for reviewing instructions, searching existing data sources, gathering and maintaining the data needed, and completing and reviewing this collection of information. Send comments regarding this burden estimate or any other aspect of this collection of information, including suggestions for reducing this burden to Department of Defense, Washington Headquarters Services, Directorate for Information Operations and Reports (0704-0188), 1215 Jefferson Davis Highway, Suite 1204, Arlington, VA 22202-4302. Respondents should be aware that notwithstanding any other provision of law, no person shall be subject to any penalty for failing to comply with a collection of information if it does not display a currently valid OMB control number. **PLEASE DO NOT RETURN YOUR FORM TO THE ABOVE ADDRESS.**

1. REPORT DATE *(DD-MM-YYYY)*	**2. REPORT TYPE**	**3. DATES COVERED** *(From - To)*
21-10-2013	Final Report	27 Sep 2012 to 27 Jun 2013

4. TITLE AND SUBTITLE
Thermospheric Mass Density Specification: Synthesis of Observations and Models

5a. CONTRACT NUMBER
FA9453-12-1-0244

5b. GRANT NUMBER

5c. PROGRAM ELEMENT NUMBER
62601F

6. AUTHOR(S)
Tomoko Matsuo and Delores J. Knipp

5d. PROJECT NUMBER
1010

5e. TASK NUMBER
PPM00014060

5f. WORK UNIT NUMBER
EF007988

7. PERFORMING ORGANIZATION NAME(S) AND ADDRESS(ES)

Regents of the University of Colorado
The Office of Contracts and Grants
3100 Marine Street, Room 479, UCB
Boulder, CO 80303-1058

8. PERFORMING ORGANIZATION REPORT NUMBER

9. SPONSORING / MONITORING AGENCY NAME(S) AND ADDRESS(ES)
Air Force Research Laboratory
Space Vehicles Directorate
3550 Aberdeen Avenue SE
Kirtland AFB, NM 87117-5776

10. SPONSOR/MONITOR'S ACRONYM(S)
AFRL/RVBXI

11. SPONSOR/MONITOR'S REPORT NUMBER(S)
AFRL-RV-PS-TR-2013-0163

12. DISTRIBUTION / AVAILABILITY STATEMENT
Approved for public release; distribution is unlimited. (377ABW-2013-0838 dtd 24 Sep 2013)

13. SUPPLEMENTARY NOTES

14. ABSTRACT

The objective of the project was to improve the thermospheric mass density specification by synthesizing a host of global observations of the thermosphere and ionosphere with a general circulation model and by characterizing the density variability associated with various external forcing. We have assimilated the neutral mass density data sampled from the Air Force (AF) High Accuracy Satellite Drag Model (HASDM) into the NCAR- Thermosphere-Ionosphere-Electrodynamics General Circulation Model using an ensemble Kalman filter assimilation procedure, and adjusted both neutral temperature and major composition mass mixing ratio globally. Global HASDM data appear to be more effective to reduce errors in the global mass density than in-situ observations obtained along satellite orbits in terms of the global neutral density specification. Among all sources of external forcing, the electromagnetic forcing in high-latitudes resulting from the solar-wind-magnetosphere interactions has the most significant impact on the mass density variability. We showed evidence that solar wind density enhancements and pressure pulses can cause intense low-energy particle precipitation and associated damping of thermospheric density response due to enhanced production of nitric oxide - an active infrared cooling agent. Ground-based indices as used by AF Space Command fail to capture these interactions in forecasting algorithms.

15. SUBJECT TERMS
thermospheric mass density, general circulation model, data assimilation, ensemble Kalman filter, solar-wind-magnetosphere interactions, high-latitude electromagnetic forcing, thermosphere density variability

16. SECURITY CLASSIFICATION OF:			**17. LIMITATION OF ABSTRACT**	**18. NUMBER OF PAGES**	**19a. NAME OF RESPONSIBLE PERSON**
a. REPORT	**b. ABSTRACT**	**c. THIS PAGE**			Dr. Chin Lin
Unclassified	Unclassified	Unclassified	Unlimited	16	**19b. TELEPHONE NUMBER** *(include area code)*

This page is intentionally left blank.

Approved for public release; distribution is unlimited.

TABLE OF CONTENTS

1. INTRODUCTION 1

2. METHODS 1

3. THERMOSPHERIC MASS DENSITY SPECIFICATION USING AN ENSEMBLE KALMAN FILTER 2

4. SPACE-BASED OBSERVATIONS RELATED TO NEUTRAL DENSITY UPHEAVALS LEAD 4

5. CONCLUSIONS 6

ACKNOWLEDGEMENTS AND DISCLAIMER 7

REFERENCES 8

This page is intentionally left blank.

1. INTRODUCTION

The density of the Earth's upper atmosphere is tenuous, yet substantial enough to exert significant drag on orbiting spacecraft and debris. Understanding this drag is complicated by the fact that this region is subject to highly variable external drivers from above and below. One of the major sources of atmospheric drag estimation errors in low Earth orbit altitudes originates from the thermospheric mass density variability. Other error sources include neutral winds and drag coefficients uncertainty as well as charged particle drag effects under some circumstances. The ionized constituents of this region also affect telecommunication and navigation, motivating numerous observational and modeling efforts since the dawn of space exploration. While the recent availability of global observations of ionospheric parameters, especially from GPS receivers on low Earthorbiting platforms, has motivated a number of attempts to assimilate ionospheric data, assimilation of sparse irregularly distributed thermospheric observations remains a daunting task.

Applications of the Kalman filter [*Kalman*, 1960] and its variants for assimilation of ionospheric observations to first principle ionospheric models have been shown to be effective [e.g., *Komjathy et al.*, 2010; *Khattatov*, 2010, and references therein]. On the other hand, thermospheric data assimilation applications have so far been limited largely by a lack of operational monitoring of thermospheric parameters. For instance, *Minter et al.* [2004] and *Codrescu et al.* [2004] presented Observing System Simulation Experiments (OSSEs) of the column-integrated ratio of atomic oxygen and molecular nitrogen. Note that OSSEs assimilate, for a given realistic observing system, synthetically generated observational data often sampled from model simulation results, in place of actually observed values.

One of the objectives of the project was to improve the thermospheric mass density specification by synthesizing a host of global observations of the thermosphere and ionosphere with a general circulation model and by characterizing the density variability associated with various external forcing. Another objective was to demonstrate how the information content of the geospace observing systems can be maximized by taking advantage of the intimate coupling between the thermosphere and ionosphere described in general circulation models (GCMs), with the help of the latest ensemble Kalman filtering (EnKF) techniques [e.g., Evensen, 1994, 2009]. Finally the third objective was to investigate the source(s) of forecasting error in 13 neutral density storms identified by AF Space Command (*B. Bowman, personal communication*).

The work comprises of two parts: Part I Thermospheric mass density specification using an ensemble Kalman filter and Part II Space-based observations related to neutral density upheavals lead. Part 1 covers the first and second objectives, whereas Part II deals with the third objective. Section 2 describes the methods. The results from Parts I and II are presented in Sections 3 and 4, respectively. Finally conclusions are given in Section 5.

2. METHODS

The global neutral mass density specification can be greatly improved by synthesizing thermospheric and ionospheric observations into general circulation model with the help of an advanced data assimilation methodology. For this purpose, we examine the utility of ensemble Kalman filtering (EnKF) techniques [e.g., *Evensen*, 1994, 2009] in assimilating a realistic set of space-based observations of the upper atmosphere into a general circulation model of the thermosphere and ionosphere. Because the neutral mass density is a derived quantity, given as a function of primary physical variables of atmospheric temperature, pressure, and compositions described in general circulation models, the problem at hand is the inverse problem of inferring these primary physical variables from indirect observations of neutral mass density and electron density. Unlike earlier applications, our approach allows simultaneous assimilation of

thermospheric and ionospheric parameters by taking advantage of the coupling of plasma and neutral constituents well described in thermosphere and ionosphere general circulation models. Specifically, the feedback between the thermosphere and the ionosphere is consistently accounted for in both the analysis and forecast steps of Kalman filtering in a systematic manner.

An EnKF assimilation system has been constructed using the Data Assimilation Research Testbed (DART) [*Anderson et al.*, 2009] and the Thermosphere-Ionosphere-Electrodynamics General Circulation Model (TIEGCM) [*Richmond et al.*, 1992], two sets of community softwares offered by NCAR. The DART implements a wide variety of ensemble filter assimilation algorithms [e.g., *Evensen*, 1994; *Keppenne and Rienecker*, 2002; *Mitchell and Houtekamer*, 2000; *Anderson*, 2001] and is carefully engineered to make it straightforward to add new compliant models. An OSSE designed for a global ionosonde network by using this EnKF system [*Matsuo and Araujo-Pradere*, 2011] suggests that the global ionospheric specification significantly benefits from better constrained thermospheric states attained through the self-consistent treatment of ionospheric and thermospheric states in assimilation algorithms.

We use an EnKF data assimilation procedure that has been constructed with the Data Assimilation Research Testbed (DART) [Anderson et al., 2009] and the thermosphere-ionosphere electrodynamics general circulation model (TIEGCM) [Richmond et al., 1992], two sets of community software offered by NCAR. Descriptions and applications of this EnKF data assimilation procedure can be found in the works of Matsuo and Araujo-Pradere [2011], and Lee et al. [2012]. We have assimilated the neutral mass density data sampled from the Air Force (AF) High Accuracy Satellite Drag Model (HASDM) into the NCAR- Thermosphere-Ionosphere-Electrodynamics General Circulation Model using an ensemble Kalman filter assimilation procedure, and adjusted both neutral temperature and major composition mass mixing ratio globally.

Perfect model experiments were used to demonstrate the effectiveness of this EnKF system to improve the neutral mass density specification from assimilation of CHAllenging Minisatellite Payload (CHAMP) in-situ neutral mass density as well as COSMIC electron density profiles. See Appendices 1 and 2 for a summary of the upper atmosphere data assimilation using the DART/TIEGCM assimilation system.

3. THERMOSPHERIC MASS DENSITY SPECIFICATION USING AN ENSEMBLE KALMAN FILTER

We investigated the impact of assimilating the neutral mass density data sampled from the Air Force (AF) High Accuracy Satellite Drag Model (HASDM) into the NCAR-TIEGCM on the global neutral mass density specification. The global HASDM mass density data from 200 to 500km, sampled with the resolution of 30^o in latitude, 45^o in longitude, and 100km in height, were assimilated every 3 hours to adjust the TIEGCM state variables including temperature and major compositions (i.e., atomic oxygen and molecular oxygen mass mixing ratio). Note that in the TIEGCM the molecular nitrogen mass mixing ratio is specified so that the sum of mixing ratio for major species (i.e., atomic oxygen, molecular oxygen, and molecular nitrogen) sums up to one. As described in Matsuo, et al., 2013, the forward (observation) operator for the neutral mass density is non-linear, and the total number of ensemble members used in EnKF experiments is 96. Filtering experiments have been conducted with the assumption of no significant model biases, and observing system simulation experiments allow us to assess the effectiveness of assimilation algorithms and strategies as well as the impact of different types of observations on the assimilation analysis. As a measure of the analysis accuracy, we use the root-mean-square deviation (RMSD) of the global neutral mass density analysis from the “true" density. (Note that a control simulation that represents the “truth” is not part of an ensemble of model forecasts used

to obtain the data assimilation analysis, even though it is simulated by using the same forecast model.) Figure 1 shows the global RMSD estimated from the entire model grid points in pressure levels 14-29 (corresponding to about 190 to 470km). The reduction of RMSD is clearly demonstrated over the course of two days. In comparison to similar filtering experiments with in-situ mass density observations from the (CHAMP) satellite, where the impact is limited to pressure levels 19-24, that assimilation of HASDM data impacts the entire TIEGCM model domain.

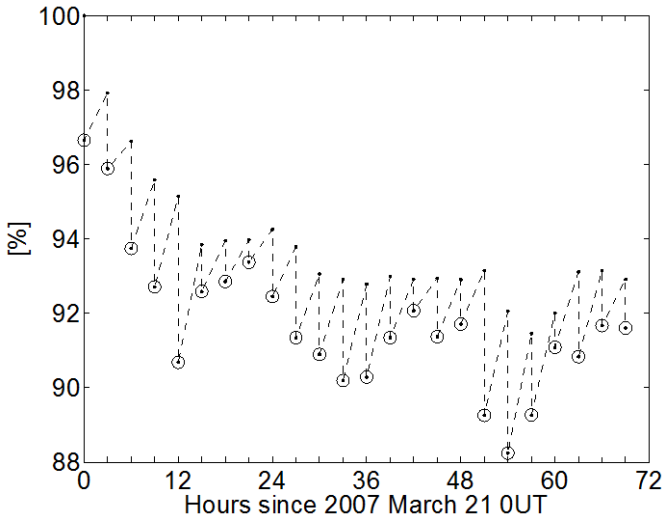

Figure 1. The global root-mean square deviation (RMSD) of the neutral mass density analysis from the "truth" is shown for March 21-23, 2007. *The global RMSD value is normalized by that of the 1st assimilation analysis to display how the RMSD varies relative to its pre-assimilation value in percentage.*

An article describing the results has been published in Journal of Geophysical Research (Matsuo et al. 2013). Matsuo (2013) presents the utility of ensemble Kalman filtering (EnKF) techniques to effectively assimilate a realistic set of space- and ground-based observations of the thermosphere and ionosphere into a general circulation model (GCM).

Since the upper atmosphere is strongly driven by external forcing, forcing parameter specifications in thermosphere-ionosphere general circulation models greatly influence the model performance and also the quality of assimilation analysis. The driver estimation described in Matsuo, et al., 2013 has been attempted with the HASDM data set, and yielded a similar result as the case with the CHAMP data. This suggests additional sampling of the neutral mass density gained by the use of HASDM may not have direct impact on estimation of the driver (i.e., solar EUV flux proxy). Driver estimation and bias correction schemes are still under investigation with the support from the AFOSR.

A manuscript describing the effort described above will be submitted to Space Weather Journal, and we are planning to transition the version of DART/TIECGM software designed to assimilate the HASDM data to AFRL for research and development efforts lead by Dr. Chin Lin.

4. SPACE-BASED OBSERVATIONS RELATED TO NEUTRAL DENSITY UPHEAVALS LEAD

We investigated the source(s) of forecasting error in 13 neutral density storms identified by AF Space Command (*B. Bowman, personal communication*). Our final study used 11 of these events; the two remaining events likely had the same source of error, described below, but were too close in time to previous storms to have the effects adequately separated. We compared the 11 "problem storm" events to 11 control events within the same time frame, 2004-2005, which appeared to be adequately forecast. Most of the problem storms were preceded by storm sudden commencements, most of the control storms were not, and thus, one implicit difference appeared to be a shock preceding the problem storms.

To further investigate similarities and differences between the two storm types, we used a superposed epoch analysis (SEA) of the density data from the CHAllenging Minisatellite Payload (CHAMP) satellite, along with several data sets from the Defense Meteorological Satellite Program F-15 spacecraft, and ground based geomagnetic indices. The SEA revealed that, despite being stronger storms by virtually every characterization, the problem storms did not achieve the same level of density upheaval as the control storms. Further, the return to normal density (lower temperature) levels was very fast in the problems storms compared to the control storms. In fact, some of the problem storms showed evidence of "overcooling." Our research breakthrough came with the acquisition of data from the Thermosphere Ionosphere Mesosphere Energetics and Dynamics *(*TIMED) Sounding of the Atmosphere using Broadband Emission Radiometry (SABER) instrument [*Russell, et al.,* 1999]. SABER's radiometer scans Earth**'** s limb from a tangent altitude of 400 km down to the Earth's surface, recording measurements of infrared (IR) radiance in spectral channels including the one for nitric oxide (NO) at 5.3 μm [*Mlynczak*, 1997].

The superposed epoch analysis shows the problem storms have a strong positive Dst initial phase (Fig. 2a) followed by a sharp downturn to a median Dst minimum = -102 nT. In comparison the control events display a slow, monotonic Dst-decrease to -81 nT. The neutral-density response for the control storms (Fig. 2b) is a slow-rise, long-duration perturbation: +120 % in 20 hours. Density rises faster in the problem storms: +83% in six hours. Despite a larger Dst excursion, the problem-storm neutral density abruptly plateaus at levels below those of the control storms. Thus, the magnitude of the neutral density response is, in general, not commensurate with the large negative values of problem-storm Dst. (A Wilcoxon rank sum test shows the control- and problem-storm NO median values to be different at the 99% significance level). The problem-storm elevated A_p index (Fig.2c) also fails to predict the plateau-response in neutral density. The root of the forecast discrepancy is the substantial NO infrared (IR) emission (Fig. 2d) during problem storms. The NO vibration-rotation bands act as an IR thermostat [*Mlynczak, et al.,* 2003]. As shown by *Maeda, et al.,* 1989, NO cooling can damp the thermospheric temperature and density response. *Lei, et al.,* 2011 report some events show "overcooling", with the thermosphere more contracted after the storm than before.

We argue that the path to the unusual NO emissions is a result of coronal mass ejection-driven sheath-enhanced storms that alter magnetosphere-ionosphere coupling via particles and Poynting flux. The main phase Poynting flux deposition is similar for problem and control storms, however DMSP data reveal excess low-energy particles during the initial and main phases of the problem storms. Comparing the DMSP <1 keV electron energy flux, we note a substantially higher flux for the problem storms than control storm within about two hours of the time Dst reaches the -75nT level (a critical storm level threshold, according to AF Space Command). These particles, along with Poynting flux, contribute to immediate upper thermosphere density uplift [*Zhang, et al.,* 2012 and *Deng, et al.,* 2013]. The ~1 keV electrons produce NO above 120 km [*Bailey, et al.,* 2002]. DMSP data also reveal an enhancement in the 1.4-4.6 keV electrons. These electrons contribute strongly to thermospheric NO production

between 100 and 110 km [*Bailey, et al.,* 2002, *Richards*, 2004]. During the 6-hr interval surrounding most problem storm onsets, DMSP ion energy flux (6.5-30 keV) also increases. *Galand, et al.,*1999 modeled a > 50% increase in NO density in the E region from this ion population. They noted that the ion-driven NO production tends to be on the nightside where the NO lifetime is many hours.

Typically, significant, storm-driven thermospheric NO enhancements develop a few hours after storm onset [*Lu, et al*., 2010]. Figure 2d shows the early increase in problem-storm NO energy flux beginning shortly after storm threshold. We believe that excess low-energy particle precipitation likely seeds the excess NO production. The fast rise of problem-storm NO emission is also aided by the increase in high-latitude Poynting flux as the IMF turns southward. Increasing temperatures associated with Joule dissipation of storm-time high-latitude Poynting flux contributes further to NO production and excitation [*Barth,* 2010].

We compared our storms to available storm lists and determined that the vast majority of our storms are associated with solar ejecta. Some Earth-arriving, solar ejecta arrive are preceded by shocks. If it exists, the sheath region of a geospace storm is a zone of compressed solar wind between the shock front and the ejecta's leading edge. Consistent with solar wind sheath structures, the distinguishing features of the problem storms are a leading period of enhanced solar wind density, n_{sw}; and a leading interval of high solar wind dynamic pressure, P_{dyn}, and enhanced interplanetary magnetic field (IMF) magnitude, B_{Tot}. *Guo, et al*., 2011 reported that solar wind coupling, and energy transfer inside the magnetosphere, differ for sheath portions of geospace storms relative to the ejecta portions. Our problem storms share many attributes of the sheath storms analyzed by the *Guo, et al.* team including the profiles of the n_{sw}, P_{dyn}, and IMF B_z. (Note: their ZEH corresponds to Dst-minimum during stronger storms.) Our control storms and their ejecta (non-sheath) storms have many common elements. Our control storms are probably slower ejecta-driven events.

Why are the low-energy particles so prominent during the problem storms? We believe there are three factors: Magnetospheric compression, solar wind/IMF pre-conditioning and solar cycle dependency. We are engaging the space weather research community in a modeling effort to address these factors. We have provided two of the magnetospheric general circulation model teams and one of the inner magnetosphere modelers with the data from three of the storms we studied. We hope to see modeling results from these events by the end of 2013.

In summary showed evidence that solar wind density enhancements and pressure pulses can lead to intense low-energy particle precipitation and an associated, but unexpected, damping of thermospheric density response. Ground-based indices, used as proxies for thermospheric energy deposition, fail to capture these interactions in forecasting algorithms. Superposed epoch comparison of a group of poorly specified neutral density storms suggests an event-chain of: 1) Multi-hour, pre-storm solar wind density enhancement, followed by solar wind dynamic pressure pulses that trigger excess low-energy particle flux to the upper atmosphere; 2) Enhanced production of thermospheric Nitric Oxide (NO) by precipitating particles and storm heating; 3) NO infrared cooling and damping of the thermosphere; 4) Mis-forecast of neutral density. In the control storms these features are absent or muted. These problem neutral-density storms reveal an element of "geo-effectiveness" that highlights competition between hydrodynamic aspects of the solar wind and other interplanetary drivers.

We provided our results to Mr Bruce Bowman of AF Space Command, who verified that the phenomena we describe has been present in a large number of storms. We have briefed our results to AFRL/RV and the IMPACT group at Los Alamos National Laboratory in April 2013 and to the Coupling Energetic and Dynamics of Atmospheric Regions (CEDAR) community in June 2013. Further we have requested additional data and event examples from AF Space Command in April 2013. We wish to determine if a proxy for the nitric oxide effect can be produced. To date we have not received this additional data.

The initial results are reported in Knipp, et al., (2013).

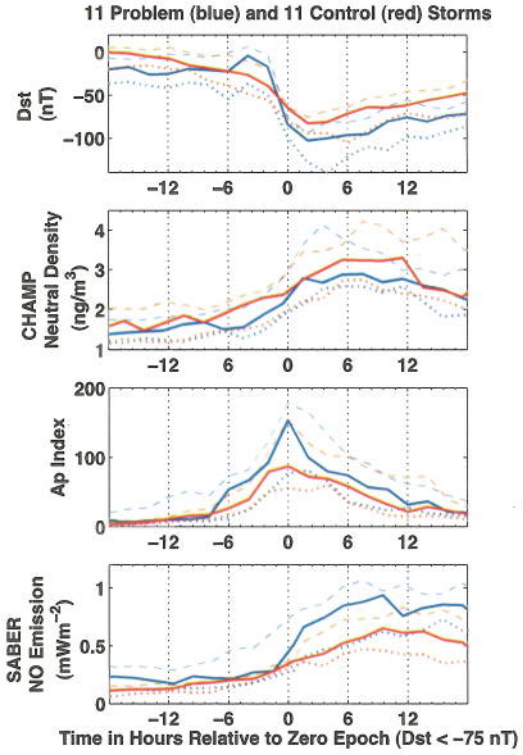

Figure 2. Superposed Epoch Profiles for 11 Problem Storms (blue) and 11 Control Storms (red). *The zero epoch time corresponds to Dst = -75 nT. Black dotted lines mark each 6 hr interval. Solid curves are median values. Dashed curves are upper quartile values. Dotted curves are lower quartile values. a) Dst index, b) CHAMP neutral density; c) A_p Index; d) SABER nitric oxide energy flux. All data are binned into 2-hour averages.*

5. CONCLUSIONS

Global HASDM data appear to be more effective to reduce errors in the global mass density than in-situ observations obtained along satellite orbits in terms of the global neutral density specification. Among all sources of external forcing, the electromagnetic forcing in high-latitudes resulting from the solar-wind-magnetosphere interactions has the most significant impact on the mass density variability. We showed evidence that solar wind density enhancements and pressure pulses can cause intense low-energy particle precipitation and associated damping of thermospheric density response due to enhanced production of nitric oxide - an active infrared cooling agent. Ground-based indices as used by AF Space Command fail to capture these interactions in forecasting algorithms.

ACKNOWLEDGEMENTS AND DISCLAIMER

This material is based on research sponsored by Air Force Research Laboratory under agreement number FA9453-12-1-0244. The U.S. Government is authorized to reproduce and distribute reprints for Governmental purposes notwithstanding any copyright notation thereon.

The views and conclusions contained herein are those of the authors and should not be interpreted as necessarily representing the official policies or endorsements, either expressed or implied, of Air Force Research Laboratory or the U.S. Government.

REFERENCES

Anderson, J. L. (2001), An ensemble adjustment Kalman filter for data assimilation, *Mon. Weather Rev.*, *129* (12), pp. 2884–2903.

Anderson, J. L., T. Hoar, K. Raeder, H. Liu, N. Collins, R. Torn, and A. F. Arellano (2009), The Data Assimilation Research Testbed: A community data assimilation facility, *Bull. Am. Meteorol. Soc.*, 90, pp. 1283–1296, doi:10.1175/2009BAMS2618.1.

Bailey, S. M., C. A. Barth, and S. C. Solomon (2002), A model of nitric oxide in the lower thermosphere, *J. Geophys. Res*., 107, A8, doi:10.1029/ 2001JA000258.

Barth, C. A. (2010), Joule heating and nitric oxide in the thermosphere, 2, *J. Geophys. Res*., 115, A10305, doi:10.1029/2010JA015565.

Codrescu, M. V., C. F. Minter, and T. J. Fuller-Rowell (2004), An ensemble type Kalman filter for neutral thermospheric composition during geomagnetic storms, *Space Weather*, *2*, S11002, doi:10.1029/2003SW000088.

Deng, Y., T. J. Fuller-Rowell, A. J. Ridley, D. Knipp, and R. E. Lopez (2013), Theoretical study: Influence of different energy sources on the cusp neutral density enhancement, *J. Geophys. Res.,* 118, pp. 2340-2349, doi:10.1002/jgra.50197.

Evensen, G. (1994), Sequential data assimilation with a nonlinear quasigeostrophic model using Monte Carlo methods to forecast error statistics, *J. Geophys. Res.*, *99*, pp. 10,143–10,162.

Evensen, G. (2009), Data Assimilation: The Ensemble Kalman Filter 2nd ed., Springer, Berlin.

Galand M., R. G. Roble, and D. Lummerzheim (1999), Ionization by energetic protons in Thermosphere-Ionosphere Electrodynamics General Circulation Model, *J. Geophys. Res.*, 104, pp. 27,973-27,990.

Guo, J., X. Feng, B. A. Emery, J. Zhang, C. Xiang, F. Shen, and W. Song (2011), Energy transfer during intense geomagnetic storms driven by interplanetary coronal mass ejections and their sheath regions, *J. Geophys. Res*., 116, A05106, doi: 10.1029/2011JA016490.

Kalman, R. E. (1960), A new approach to linear filtering and prediction problems, *J. Basic Eng.*, *82*(D), pp. 34–45.

Khattatov, B. (2010), Assimilation of GPS soundings in ionospheric models, in Data Assimilation: Making Sense of Observations, edited by W. Lahoz, B. Khattatov, and R. Ménard, Springer-Verlag, Berlin, pp. 599-622.

Keppenne, C. L. and M. M. Rienecker (2002), Initial testing of a massively parallel ensemble Kalman filter with the poseidon isopycnal ocean general circulation model, *Mon. Weather Rev.*, *130*(12), pp. 2951–2965, doi:10.1175/1520-0493.

Knipp, D., L. Kilcommons, L. Hunt, M. Mlynczak, V. Pilipenko, B. Bowman, Y. Deng, and K. Drake (2013), Thermospheric damping response to sheath-enhanced geospace storms, Geophys. Res. Lett., 40, doi:10.1002/grl.50197.

Komjathy, A., B. Wilson, X. Pi, V. Akopian, M. Dumett, B. Iijima, O. Verkhoglyadova, and A. J. Mannucci (2010), JPL/USC GAIM: On the impact of using COSMIC and groundbased GPS measurements to estimate ionospheric parameters, *J. Geophys. Res.*, *115*, A02307, doi:10.1029/2009JA014420.

Lee, I. T., T. Matsuo, A. D. Richmond, J. Y. Liu, W. Wang, C. H. Lin, J. L. Anderson, and M. Q. Chen (2012), Assimilation of FORMOSAT-3/COSMIC electron density into thermosphere/Ionosphere coupling model by using ensemble Kalman filter, *J. Geophys. Res*., 117, A10318, doi:10.1029/2012JA017700.

Lei, J., J. P. Thayer, G. Lu, A. G. Burns, W. Wang, Eric K. Sutton, and Barbara A. Emery (2011), Rapid recovery of thermosphere density during the October 2003 geomagnetic storms, *J. Geophys. Res.*, 116, A03306, doi: 10.1029/2010JA016164.

Lu, G., M. G. Mlynczak, L. A. Hunt, T. N. Woods, and R. G. Roble (2010), On the relationship of Joule heating and nitric oxide radiative cooling in the thermosphere, *J. Geophys. Res.,* 115, A05306, doi: 10.1029/2009JA014662.

Maeda, S., T. J. Fuller-Rowell, and D. S. Evans (1989), Zonally averaged dynamical and compositional response of the thermosphere to auroral activity during September 18-24, 1984, *J. Geophys. Res.*, 94, A(12), doi:*10.1029/JA094iA12p16869*.

Matsuo, T. (2013), Upper atmosphere data assimilation with an ensemble Kalman filter, AGU Geophysical Monograph Series, in press.

Matsuo, T. and E. A. Araujo-Pradere (2011), Role of thermosphere-ionosphere coupling in a global ionospheric specification, *Radio Science*, 46, RS0D23, doi:10.1029/2010RS004576.

Matsuo, T., I.-T. Lee, and J. L. Anderson (2013), Thermospheric mass density specification using an ensemble Kalman filter, *J. Geophys. Res. Space Physics,* 118, pp. 1339-1350, doi:10.1002/jgra.50162.

Minter, C. F., T. J. Fuller-Rowell, and M. V. Codrescu (2004), Estimating the state of the thermospheric composition using Kalman filtering, *Space Weather*, *2*, S04002, doi:10.1029/2003SW000006.

Mitchell, H. L. and P. L. Houtekamer (2000), An adaptive ensemble Kalman filter, *Mon. Weather Rev.*, *128*(2), pp. 416–433, doi:0.1175/1520-0493.

Mlynczak, M. G. (1997), Energetics of the mesosphere and lower thermosphere and the SABER Experiment, *Adv. Space Res.* Vol. 20, No. 6, pp. 1177-1183.

Mlynczak, M. G., F. J. Martin-Torres, J. Russell, K. Beaumont, S. Jacobson, J. Kozyra, M. Lopez-Puertas, B. Funke, C. Mertens, L. Gordley, R. Picard, J. Winick, P. Wintersteiner, and L. Paxton (2003), The natural thermostat of nitric oxide emission at 5.3 μm in the thermosphere observed during the solar storms of April 2002, *Geophys. Res. Lett.*, 30(21), doi: 10.1029/2003GL0 17693.

Richards, P. G. (2004), On the increases in nitric oxide density at midlatitudes during ionospheric storms, *J. Geophys. Res.,* 109, A06304, doi: 10.1029/2003JA010110.

Richmond, A. D., E. C. Ridley, and R. G. Roble (1992), A thermosphere/ionosphere general circulation model with coupled electrodynamics, *Geophys. Res. Lett.*, 19, pp. 601-604.

Russell, J. M., M. G. Mlynczak, L. L. Gordley, J. J. Tansock, Jr., and R. W. Esplin (1999), Overview of the SABER experiment and preliminary calibration results, *Proc. SPIE* 3756, Optical Spectroscopic Techniques and Instrumentation for Atmospheric and Space Research III, 277 (October 20, 1999); doi:10.1117/12.366382.

Zhang, B., W. Lotko, O. Brambles, M. Wiltberger, W. Wang, P. Schmitt, and J. Lyon (2012), Enhancement of thermospheric mass density by soft electron precipitation, *Geophys. Res. Lett*., 39, L20102, doi:10.1029/2012GL053519.

DISTRIBUTION LIST

DTIC/OCP
8725 John J. Kingman Rd, Suite 0944
Ft Belvoir, VA 22060-6218 1 cy

AFRL/RVIL
Kirtland AFB, NM 87117-5776 2 cys

Official Record Copy
AFRL/RVBXI/Dr. Chin Lin 1 cy